

Basic Structures of Matter – Supergravitation Unified Theory Based on an Alternative Concept of the Physical Vacuum

Stoyan Sarg (Sargoytchev), PhD

York University, Toronto, Ontario, Canada

s.sarg@helical-structures.org, sto.sarg@gmail.com

Abstract: The Basic Structures of Matter - Super Gravitation Unified Theory (BSM-SG) unveils the relation between the forces in Nature by adopting the following framework:

- Empty Euclidian space without any physical properties and restrictions
- Two fundamental particles of superdense matter with parameters associated with a Planck's scale
- A Fundamental law of Super Gravitation (SG) - an inverse cubic law valid in pure empty space.

An enormous abundance of these two particles, with vibrational energy beyond some critical level, is able to congregate into self-organized hierarchical levels of geometrical formations, based on the fundamental SG law. A self-organized process leads deterministically to creation of space with quantum properties (known as physical vacuum) and a galaxy as observable matter. All known laws of Physics are embedded in the underlying structure of the physical vacuum and the structure of the elementary particles. The fundamental SG law is behind the gravitational, electric and magnetic fields and governs all kinds of interactions between the elementary particles in the space of physical vacuum.

Keywords: Physical vacuum, space-time, unified theory, quantum gravitation, zero point energy, cosmological redshift,

Introduction. The contemporary theoretical Physics is plagued of problems, affecting the fields of Particles Physics, Quantum Mechanics, Theory of Relativity and Cosmology. Most of the physical models in different fields are more mathematical, than physical. When trying to connect them together, they are contradictable, so they barely give the real picture of the microcosmos and Universe. The Big Bang model also has numerous problems, indicating that the galactic redshift might not be of Doppler type. One of the recent proofs is the distribution of the quasars showing that they are not at the "edge" of the observable Universe [1]. The main reason for all these problems is in the concept of the space, known as a physical vacuum, adopted 100 years ago.

James Clerk Maxwell, the farther of Modern Physics developed the Classical Electrodynamics with the assumption of material Ether. This is evident from his famous work "A Treatise on Electricity and Magnetism, section "A medium is necessary", p. 493 [2]. After the inconclusive Michelson-Morley experiment, Einstein formulated in 1905 his postulate of Relativity, opposing the idea of the Ether, but after he developed the General Relativity in 1920, he reversed partly his opinion claiming that the Ether is necessary [3]. At the same time, he still envisioned the Ether as a not material substance, which diverted the search from the direction envisioned by Faraday, Maxwell, Lord Kelvin and many others famous scientists. The only argument of Einstein against the material Ether presented in his book "Sidelights of Relativity" [3] is that "neither Maxwell nor his followers succeeded in elaborating mechanical model for the ether". Einstein, however, did not present any proof that the concept of material Ether is impossible. Presently, after the proof that different types of laboratory experiments detect our absolute motion through some real substance [4-13], it was understood that the Michelson-Morley experiment had a methodological error. Additionally, the Casimir's forces has been discovered 35 years later than Einstein's statement, but nobody so far guessed, that they might be a signature of the most fundamental law in Nature – a Law of Supergravitation. This law namely allows unveiling the superfine substance of the space, in order to go beyond the Newton's laws of gravity and inertia and the Einstein's theory of Relativity. While the search of correct physical model of this substance has been officially abandoned, it was the starting point of the "Basic Structures of Matter – Supergravitation Unified Theory" (BSM-SG) [14-25].

Extensive analysis of phenomena from different fields of physics led to the development of unified theory with a following framework:

- **Two spherical superdense indestructible fundamental particles (FPs)** of two different substances of intrinsic matter with a radius ratio of 2:3 and different densities. The bell-shape curve radial dependence of their density permits a central of mass type of vibrations of the FP individually and in 3D formations. They are able to vibrate at extremely high proper frequency, the average (for both types FPs) value of which is associated with the Planck's frequency:

$$[(2\pi c^5)/(Gh)]^{1/2} = 1.855 \times 10^{43} \text{ (Hz)} \quad (1)$$
- A fundamental law of Super Gravitation (SG), governs the interactions between FPs in a **classical void space**, according to which FPs from the same substance interact by a force inverse proportional to the cube of the distance. The SG law in empty space is given by

$$F_{SG} = G_O \frac{m_{01}m_{02}}{r^3} \quad (2)$$

where: F_{SG} is the SG force, m_{01}, m_{02} intrinsic matter mass, r – distance; G_O – is a SG constant, which is different for both matter substances and may change the sign for a case of imbalanced geometrical formation

- **Vibrational energy and SG law:** FPs preserve a limited freedom of vibrations in geometrical formations from the same type of substance. In a complex 3D structure, FPs may vibrate within a saturation limit – an energy well of the structure. SG law could be associated with the necessary energy for filling the energy well. The SG attraction between FP formations of different substances in a uniform lattice (discussed later) may not be so strong or could even convert to repulsion at different mutual distance due to a different time constants of both FPs.

The suggested physical model allows using a classical approach in a real 3-dimensional space with unidirectional time, so the principles of causality, objectivity and logical understanding are completely preserved. The derived physical models exhibit excellent properties when they are applied for analysis of numerous experiments and observations from the range of particle physics to cosmology. This is demonstrated in BSM-SG theory. Based on that analysis, a cosmological scenario is presented in Chapter 12, which can be briefly summarized as follows:

The enormous abundance of these two Fundamental Particles with energy above some critical level, driven by the SG law into self-organized hierarchical level of 3D formations, leads deterministically to creation of space with quantum properties – physical vacuum and elementary particles forming the observable matter of an individual galaxy.

Under SG law, the matter is organized in hierarchical levels of 3D formations based on 3D geometry. Fig. 1, shows consecutive types of 3D formations at the lowest level of hierarchical order. They are denoted as Tetrahedron (TH), Quasipentagon (QP) and Quasiball (QB).

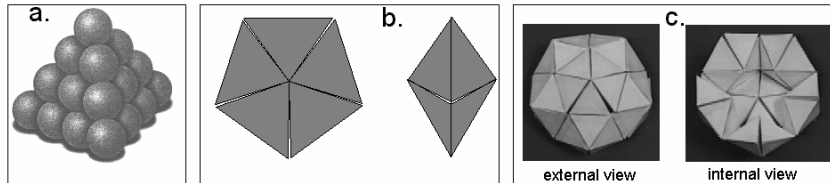


Fig. 1. Structures of lowest level. a. Tetrahedron (TH), b – Quasipentagon, c. – Quasiball (QB)

The next order, contains the same type of formations, while the TH is formed by QBs of previous order. The rotational internal SG modes are strongest at TH with SG field stronger at the edges. This keeps the formations and constant number between formations of same type and order. The SG modes in QP exhibit an axial anisotropy due to its geometrical shape. The gaps between the THs in QP are combined in a common gap of 7.355^0 , which is preserved in QB. This allows a left or right hand twisting of the QB – this is a **lowest level memory carrying the chirality (handedness)**. The sectional view of QB shows that this formation encloses an internal empty space.

1 QB = 12 QP = 60 PT – equation of constant intrinsic matter quantity (valid for any upper order formations of the same type)

Fig. 2. illustrates the hypothetical consecutive phases of the primordal matter evolution from both FPs leading to crystallization of elementary particles. This process takes place in a hidden phase of evolution of every individual galaxy. before it is born by explosion. whose detectable signature is

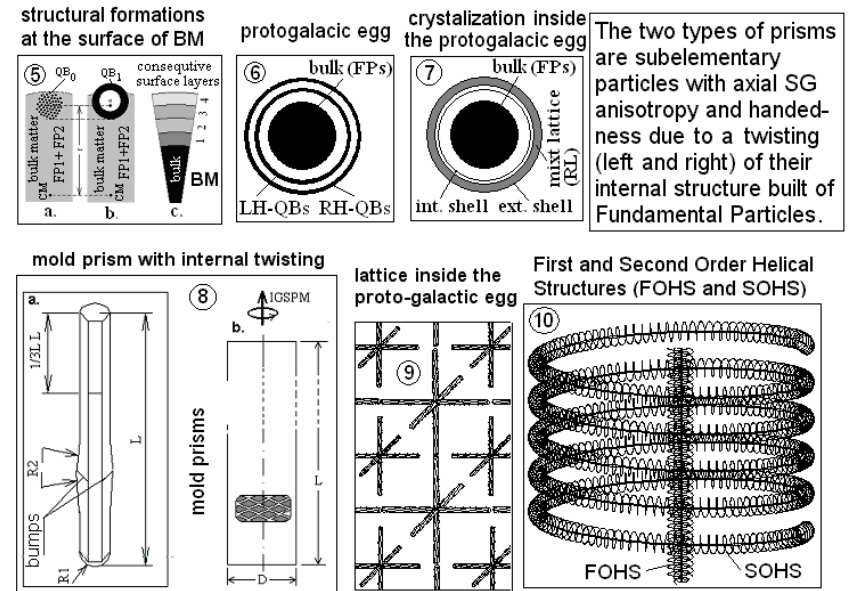


Fig. 2. Phases and structural 3D formations at lower level of matter organization leading to creation of the particles called prisms, from which the superfine structure of the space and elementary particles are built.

The matter evolution following the process of particle crystallization is an explosion of the protogalactic egg in which a new galaxy is born in the void space occupied by the previously collapsed one. The free prisms form a Cosmic Lattice (CL), while the stable particles - protons, neutrons and electrons firstly form simple atoms, such as hydrogen, deuterium, tritium, helium and also the first molecules. The newborn space has all known properties of the physical vacuum and may have a higher Zero Point Energy, which will be detected as a blue galactic shift (for example, Andromeda galaxy).

The properties of the CL space are following:

- The CL space is formed of alternatively arranged CL nodes made of 4 prisms of the same type, which have intrinsically small inertia in a void space
- The distance between the CL nodes is kept by the SG forces the sign and strength of which depend on the distance due to the different time constants of the two FPs .
- CL space possesses quantum and space-time properties and Zero Point Energy, which includes two components: a Static (strong one) and a Dynamic (weak one)
- The SG field between the elementary particles in CL space is propagated by the **abcd** set of axes (see Fig. 3) of the CL nodes and appears as a Newtonian gravitation
- The Electrical and Magnetic fields are type of CL space modulation, based on the dynamic properties of the CL nodes involving mostly momentums along the **xyz** set of axes.

Fig. 3 illustrates the CL node, formed by 4 prisms of the same type of FP's held by SG forces. Its dynamics under SG law is described by two vectors: Node resonance momentum (NRM) and Spatial Precession Momentum (SPM). The hodograph of NRM (cycle) is an open flat curve. A large number of NRM cycles forms a closed surface called Quasisphere with 6 bumps (along xyz axes) and 4 depressions (along abcd axes). MQ is a magnetic Quasisphere (with central symmetry), while EQ is an Electrical Quasisphere involved in Electrical lines. MQ (or EQ) involved in magnetic (or electrical lines) are phase synchronized, but their SPM frequency is different. The energy of EQ is larger than MQ. The photon is a wave with a helical configuration involving EQs and boundary of MQs. The MQs at the boundary assure the preservation of the quantum energy of the photon during its propagation. During this propagation the energy momentum from every CL node included in the wavetrain transfers to a neighboring one for one NRM cycles – this defines the velocity of light. The transfer through a large number on CL nodes is in a helical path with a step defining the photon wavelength.

The velocity of light is additionally strongly stabilized by the effect of self synchronization between the CL nodes, which is with the SPM (Compton's) frequency and defines the permeability and permittivity of the physical vacuum (Chapter 2 of BSM-SG).

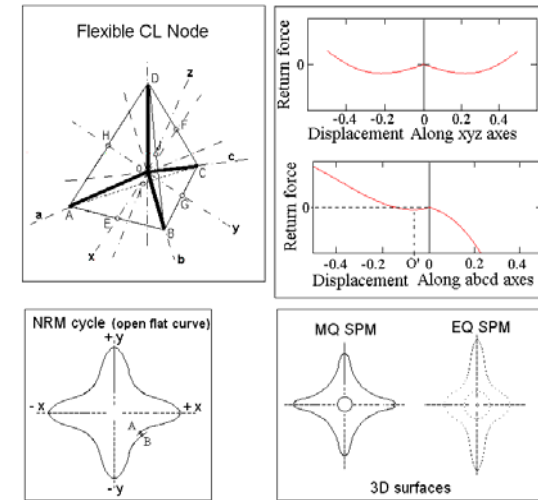


Fig. 3. CL node and its dynamics under SG law

The **Elementary particles** are built of prisms arranged in **helical structures** in a crystallization process preceding the birth of the galaxy.

The Electron is a one coil of First Order Helical Structure (FOHS) - an oscillating 3-body system with two proper frequencies [21]. The first one is the Compton frequency equal to the SPM frequency of the CL node. Fig. 4 shows its overall shape and dimensions, internal lattice structure (impenetrable for CL structure) and its modulation on the CL nodes, appearing as a charge.

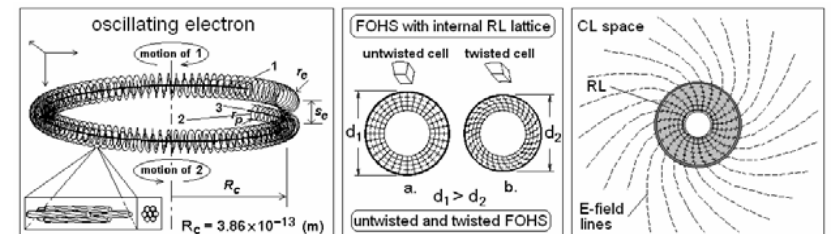


Fig. 4. Electron with its internal lattice modulating the CL space. Calculated dimensions: (m): $R_c = 3.86 \times 10^{-13}$; $r_e = 8.8428 \times 10^{-15}$; $r_p = \frac{2}{3} r_e$

The fine structure constant is embedded in the helical step of the electron:

$$s_e = (\alpha c/v_c)(1-\alpha^2)^{1/2} = 2r_e = 1.7706 \times 10^{-14} \quad (m) \quad (3)$$

The **denser internal lattice of FOHS** modulates the CL space, creating aligned EQ SPM – **electrical field lines**. When moving and rotating, they cause formations of loops of phase synchronized MQs – **magnetic lines**.

Confined motion: The screw-like motion of the rotating and oscillating electron and its interaction with the SPM frequency of the CL nodes causes a confined motion with preferred velocities, corresponding to $(13.6/n)$ eV, where n matches the principal quantum number of the Bohr atomic model. In a closed loop motion, n defines the real length of the quantum orbit [21], because the loop length contains a whole number of quantum magnetic lines - Compton's wavelength (See §7.7.1, Chapter 7 of BSM-SG).

Using the unveiled structure and oscillating properties of the electron, the following physical parameters of the CL space are derived:

Static CL pressure, P_S : defines the Newtonian mass of elementary particle (Equation 5) as a pressure exercised on its impenetrable internal lattice

$$P_S = \frac{m_e c^2}{V_e} = \frac{g_e h v_c^4 (1-\alpha^2)}{\pi \alpha^2 c^3} = 1.3735 \times 10^{26} \quad (N/m^2) \quad (4)$$

$$m = (P_S/c^2)V_H \quad (kg) - \text{mass (Newtonian) equation of the electron} \quad (5)$$

where: V_e – volume of impenetrable internal lattice of the electron

Partial CL pressure, P_P : related to the inertial properties of the elementary particles in CL space at their confined motion

$$P_P = P_S \alpha v/c \quad (N/m^2) \quad \text{where: } U - \text{is velocity} \quad (6)$$

Dynamical CL pressure, P_D : - exercised on atoms and molecules by ZPE waves responsible for equalization the CL space background energy.

$$P_D = \frac{h v_c}{c S_e} = \frac{g_e h v_c^3 (1-\alpha^2)}{\pi \alpha c^3} = 2.0258 \times 10^3 \quad \left(\frac{N}{m^2 Hz}\right) \quad (7)$$

The signature of P_D is the observed Cosmic Microwave Background (CMB). Therefore, **the estimated temperature of 2.72K** (by fitting of CMB to a blackbody curve) **in fact is a CL space background parameter**. The derived theoretical expression (see Chapter 5 of BSM-SG) is:

$$T = \frac{N_A^2}{S_W} \frac{h v_c (R_C + r_p)^3 L_{PC}^2}{2 c R_C r_e R_{ig}} \frac{\mu_e}{\mu_n} = 2.6758 K \quad (8)$$

Other estimated CL space parameters:

CL node distance (at xyz axes) $\sim 1.0975 \times 10^{-20}$ (m),

NRM (resonance) frequency: 1.0926×10^{29} (Hz)

SPM frequency = Compton's frequency (known): 1.2356×10^{20} (Hz)
ZPE-S = 1.373×10^{26} (J) – Static Zero Point Energy of space (hidden energy of non EM type – a primary source of the nuclear energy (BSM, Chapter 5)

Using the particle data and the derived mass equation, the internal structure of the proton and neutron is identified, as shown in Fig 5. The calculated dimensions are verified by analysis of atoms connected in molecules and by comparison with experimentally obtained bond lengths.

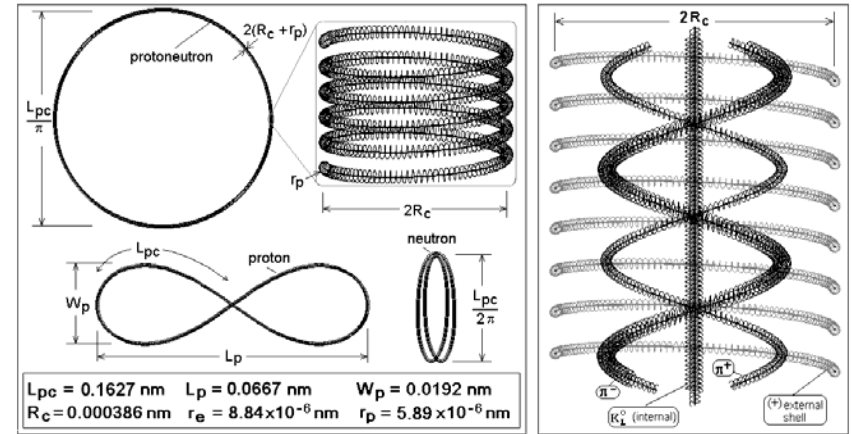


Fig. 5. Overall shape and internal structure of the proton and neutron with calculated dimensions

The proton-neutron with a shape of torus is unstable in CL space. The proton has the same structure but twisted in a shape of 8, as shown in Fig. 5 so it is stable. The neutron has the same structure but is almost double folded, as shown in Fig. 5 and it is more stable when it is over the proton forming a deuterium, as shown in Fig. 6. The CL space modulation from the proton (CL node dynamics) appears as a charge, but for the neutron it is compensated in the far field due to the symmetry of its internal structure. The neutron's charge appears "locked" in a proximity, but it provides a small magnetic field, when in motion. This is the reason for the magnetic moment of the neutron. Fig. 6 shows the spatial arrangement of the protons and neutrons in the atomic nuclei.

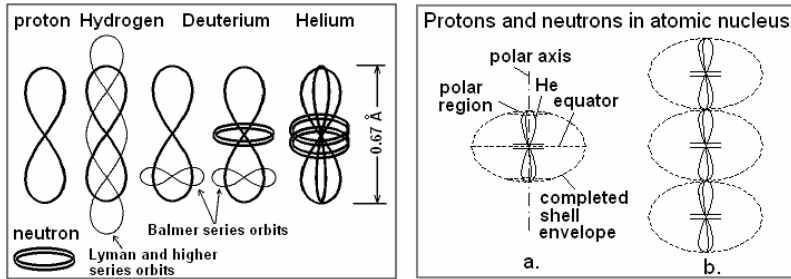
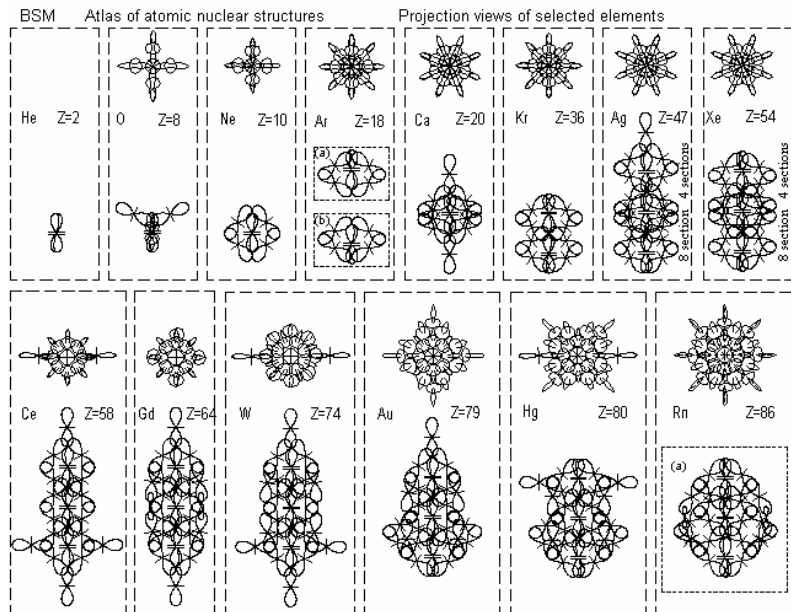


Fig. 6. Protons and neutrons arrangement in atomic nuclei

The unveiled nuclear structures of stable elements of the Mendeleev Periodic Table are presented in the Atlas of Atomic Nuclear Structures – Appendix A of the BSM-SG book. The protons and neutrons are shown by symbols for simplifying the drawings, but 2D projections for each of them can be made as for some selected elements shown in Fig. 7. For a neutral atom each proton has own bound electron, so the positions of the electron quantum orbits are completely defined by the nuclear structure. The atomic nuclei are in fact slightly twisted due to the twisted 3D overall shape of the proton.



Note: (a) and (b) are polar sections of the nucleus with two selected planes. The angle between them is 22.5°

Fig. 7. 2D projections of some selected atomic nuclei.

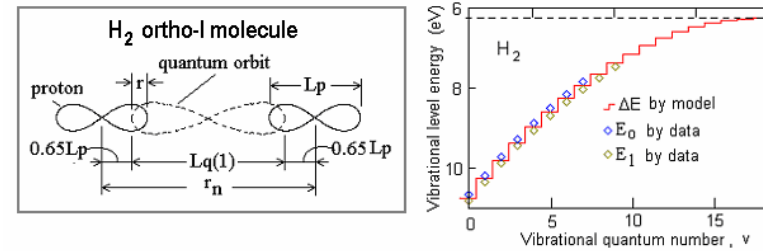


Fig. 8. A physical model of the H₂ – ortho molecule

The parameters of H₂ molecule (shown in Fig. 8) were obtained by using some optical and photoelectron spectra. It permitted the derivation of Eq. (9) for vibrational levels, plotted in Fig. 7 together with levels from optical spectrum and obtaining the value of one important factor of the SG law denoted as C_{SG} (Chapter 9). H₂ – ortho system participates in chemical bonds.

$$E_v = \frac{C_{SG}}{q[[L_q(1)(1 - \alpha^4 \pi \Delta^2)] + 0.6455L_p]^2} - \frac{2E_q}{q} - \frac{2E_k}{q} \quad (9)$$

$$C_{SG} = G_0 m_0^2 = (2h\nu_c + h\nu_c \alpha^2)(L_q(1) + 06455L_p)^2 = 5.2651 \times 10^{-33} \quad (10)$$

$$C_{SG} / Gmp^2 = 2.82 \times 10^{31} \quad (11)$$

where: q – electron charge, $L_q(1)$ – quantum orbit length for electron velocity of 13.6 eV, L_p – proton length, Δ - vibration level, $E_q = 511$ KeV, E_k – electron kinetic energy, ν_c – Compton frequency, α - fine structure constant, G_{SG} – SG gravitational constant, m_0 – SG mass of the proton (also neutron).

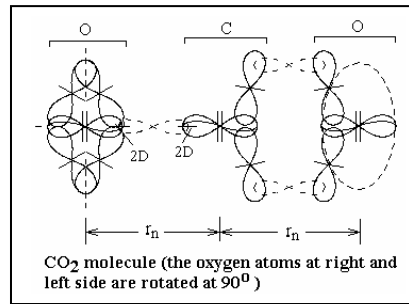
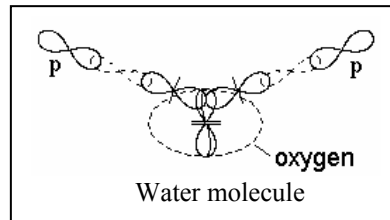
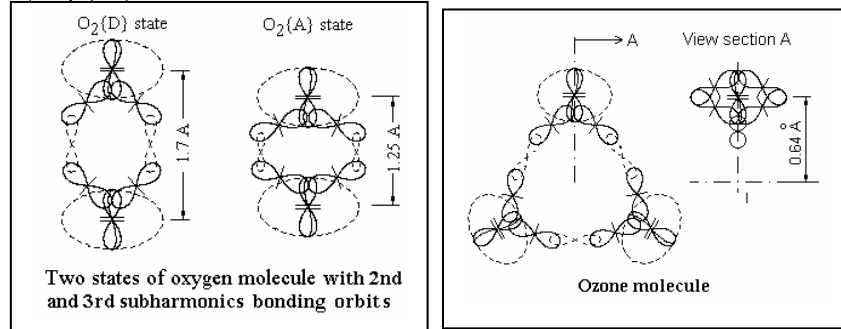
The ratio (11) shows that the FPs and their formations are much denser than the atomic matter. The derived factor C_{SG} is additionally verified by calculating of the binding energy between the proton and neutron in the Deuterium (Chapter 6 of BSM-SG, p. 6-52). Using a simplified approximated model the calculated binding energy is 2.145 (MeV), which is quite closer to the experimentally obtained value of 2.2245 (MeV).

The analysis and the derived structure of simple molecules indicates that the H₂ – ortho molecule is imbedded as a chemical bond system in the molecules, having vibrational rotational spectra. An equation similar as (9) was derived also for D₂ molecule, which is a more common system in the chemical bonds. For other simple diatomic molecule a universal expression (12) for internuclear distance r_n , is derived. In §9.75.D (Chapter 9 pf BSM) it is shown that the vibrational range distance is negligible in comparison to the internuclear distance r_n , due to the involved SG law (this is unresolvable discrepancy between the Quantum Mechanical models and the observations).

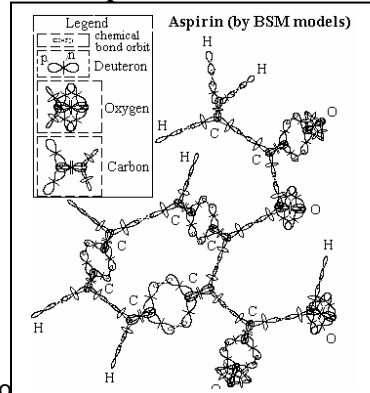
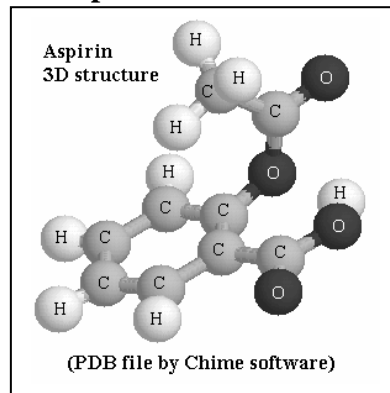
$$r_n = (A - p)[(2\alpha C_{SG}) / (pB_{D_2}(n))]^{1/2} \quad (12)$$

where: A - mass in atomic mass unit (per one atom), p - number of protons involved in the chemical bond (per one atom), n - subharmonic quantum number of the orbit, B_{D_2} - energy of D_2 bonding system; α - fine structure constant

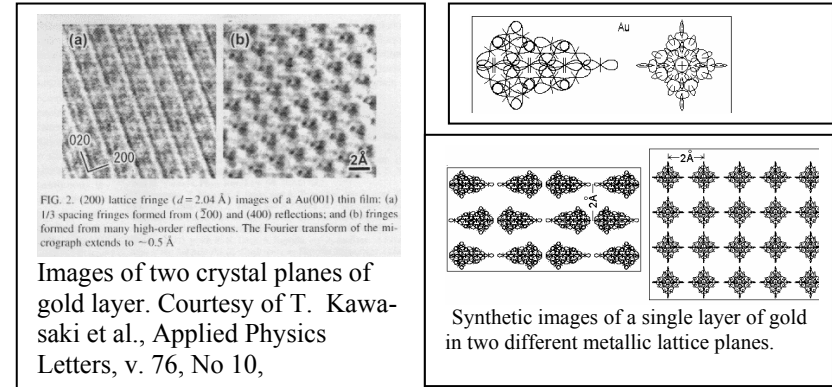
BSM atomic models for simple molecules (obtained by analysis of photoelectron and optical spectra and calculating the internuclear distance by Eq. (12).



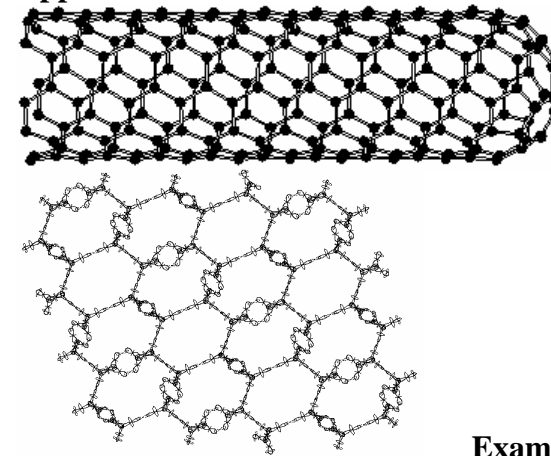
Example of BSM atomic models for complex molecules:



Atoms in metallic lattice



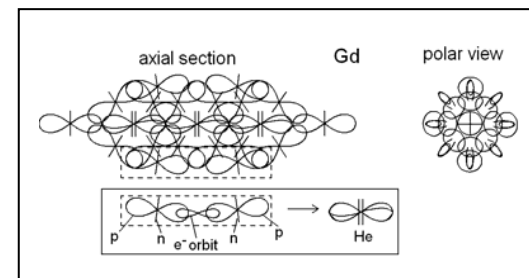
Application of the BSM atomic models in nanotechnology



Axonometric view of a single-walled carbon nanotube

An axonometric view of a synthetic image of the carbon sheet using BSM atomic models

Example of α decay



α radioactive decay of Gd as a fusion at room temperature

$D + D \rightarrow He$

Inertia beyond the Newton's first and second laws (Chapter 10 of BSM)

The CL node flexibility allows it to be partly folded and deviated when the electron (and any elementary particle) moves through the CL space.

Multiplying Eq. (6) by the volume of the electron's structure we obtain

$$\vec{E}_{IFM} = P_p V_e = h v_c \alpha \vec{v} / c \quad [\text{J}] - \text{for a moving electron} \quad (13)$$

The vector E_{IFM} , called an Inertial Force Moment, allows estimating the deviation energy of the folded CL nodes, displaced from their normal positions at velocity U . It can be scaled for a moving proton (neutron) using the volume ratio between FOHSs of electron and proton (equal to their mass ratio). Eq. (14) is valid for a moving proton (neutron), while Eq. (15) for a moving atom with an atomic number A (u – is atomic mass unit)

$$\vec{E}_{IFM} = (m_p c \alpha) \vec{v} - \text{for a proton}; \quad \vec{E}_{IFM} = (m_n c \alpha) \vec{v} - \text{for a neutron} \quad (14)$$

$$\vec{E}_{IFM} = (c \alpha A u) \vec{v} - \text{for a moving atom} \quad (15)$$

The vector E_{IFM} permits to transfer the concept of the deviated node energy to a solid object. The analysis of the force moment of a real body with a mass m in a free fall motion under acceleration g leads to the expression:

$$\Delta E_{IFM} = \alpha c m g$$

The gravitational potential in the initial moment is:

$$U_G = G M m / R$$

Dividing ΔE_{IFM} on U_G we get

$$U_G / \Delta E_{IFM} = R / (\alpha c) \quad [\text{s}] \quad (16)$$

Scaling Eq. (15) for a Compton's time interval we get a quite close value to s_e , (see Eq. (3)). $R = \alpha c / v_c = 1.7706 \times 10^{-14} (m) \approx s_e = 2r_e$. (17)

Conclusion: The CL nodes folds and deviate around the small electron radius - an indication of its inertial interaction with the CL space. The derived result is transferable to any elementary particle, by normalizing their mass to the mass of the electron.

Fig. 9 shows a plot of Eq. (15) for solar planets and moons, denoted by numbers. All points lie on a predicted theoretical line, however, Mercury (number 15) appears in a reversed order in respect to others. To investigate this, the planetary and moon masses are plotted versus their volume as shown in Fig. 10, while an expanded version is shown in Fig. 11. The broken trend

coincides with the appearance of magnetic field in planets or moons, whose physical explanation from a new point of view is discussed in Chapter 10.

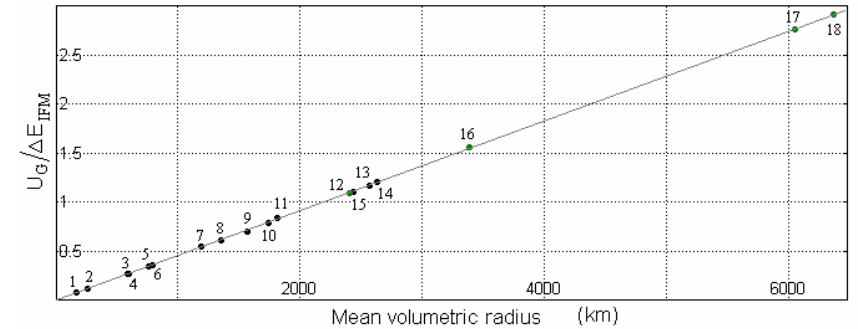


Fig. 9. Plot of Eq. (15) for solar planets and moons

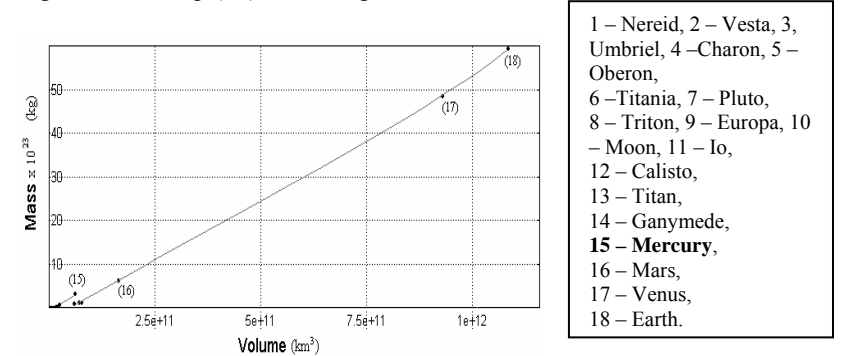


Fig. 10. Planetary and moon masses versus their volumes

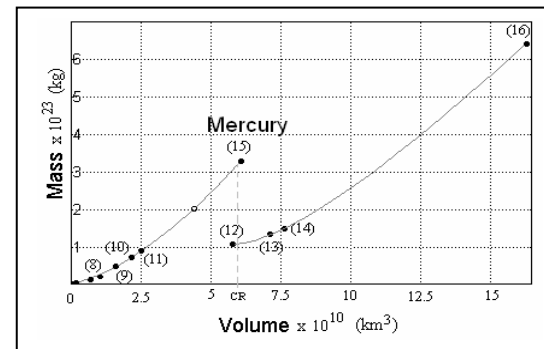


Fig. 11. Expanded view of the broken trend

The analysis led to **formulation of the following hypothesis:**

Protons and neutrons in the central region of heavy astronomical body may crush forming a denser bunch of straight FOHSs. Such formation may cause a strong magnetic field. This is in agreement with the formations of pulsars from collapsing stars, discussed in Chapters 10&12 of BSM-SG.

The square of the ratio between the E_{IFM} and the orbital kinetic energy of a planet of the solar system is

$$\left[\frac{E_{IFM}}{E_K} \right]^2 = \frac{4\alpha^2 c^2}{GM_S} r = C_E r \quad (18)$$

For a solar mass $M_S = 1.9891 \times 10^{30} (kg)$, one obtains $C_E = 1.44238 \times 10^{-7}$.

Fig. 12 shows a plot of $[E_{IFM}/E_K]^2$ versus the mean orbital radius r for the solar planets. The slop of the fitted line gives a data value of C_E , which differs only by 0.06% from the theoretical one, given by Eq. (18).

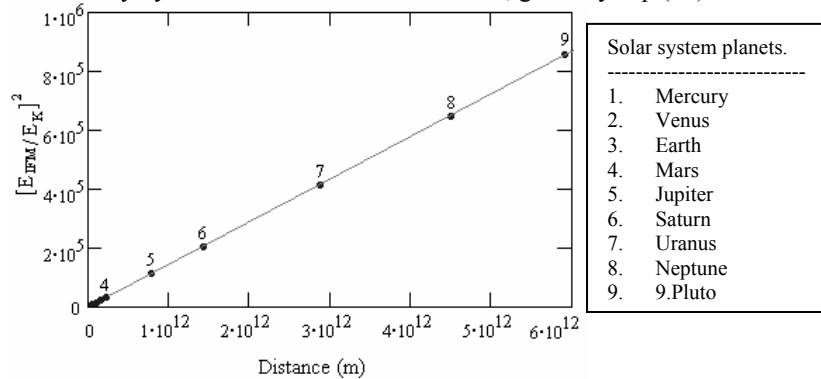


Fig. 12 $[E_{IFM}/E_K]^2$ versus the mean orbital radius r for the solar planets.

Conclusions:

The expressions from (14) to (18) and corresponding plots indicate that the **fine structure constant (α) plays an important role in the inertial interactions**. Indeed, dividing Eq.(6) on Eq. (4) one obtains an expression that depends only on α for a case of optimal confined electron motion (13.6 eV).

$$P_p / P_s = \alpha^2 / \sqrt{1 - \alpha^2} \quad (19)$$

(For confined motion with suboptimal electron velocities for energies of 3.41 eV and 1.51 eV, the ratio (19) is divided, respectively, on 2 and 4).

Theoretical and experimental results about the fine structure constant α and the Gravitational constant G

Due to different strength of the return forces along the two sets of the CL node axes and the asymmetry along the $abcd$ set, the single NRM cycle is almost a flat but open 3D curve, as shown in Fig. 3. If the hodograph of the NRM vector circumscribes a closed 3D surface for 137 NRM cycles plus a small fraction, one obtains the formula (20) matching accurately the value of α given by CODATA 98 (See Chapter 12 of BSM-SG, p. 12-16).

$$\alpha = 2 / [(n^2 + 2\pi^2)^{1/2} + n] = 7.29735194 \times 10^{-3} \quad (20)$$

$$\alpha = 7.2973525 \times 10^{-3} \text{ - experimental value by CODATA 98}$$

The fine structure constant, α , is widely apparent in Particle Physics experiments, Quantum Mechanics and even in the mechanics of celestial bodies as shown in the above presented analysis. It is reasonable to search a direct relation between this fundamental parameter and the Gravitational constant, whose value was only experimentally determined. Among the most promising theoretical expression is one suggested by A. I. Zakazchikov, showing a good match with a number of physical constants [26].

$$G_{theor} = \frac{c^5}{\pi \hbar v_c^2} \left(\frac{\alpha^3}{4} \right)^6 = 6.66294 \times 10^{-11} \quad (21)$$

$$G = 6.6742 \times 10^{-11} (m^3 kg^{-1} s^{-2}) \text{ - by NIST CODATA} \quad (22)$$

Now let us use the presented above analysis of the solar system. Fitting the data shown in Fig. 23 to a robust line, we obtain the value of $C_E = 1.44238 \times 10^{-7}$. Then we obtain an expression of the gravitational constant, G_{SS} , for the Solar system in which α participates.

$$G_{SS} = \frac{4\alpha^2 c^2}{C_E M_S} = 6.66873 \times 10^{-11} \quad (23)$$

We see that G_{SS} is much closer to G_{theor} (accuracy of 0.004%), than to the G , while the last one is experimentally determined for Earth environments. According to the presented physical model, α should be a stable constant, while the gravitational constant G may slightly vary, depending on the mass of the astronomical body. This is in good agreement with the BSM-SG interpretation of the General Relativity, and might help understanding some local variations of G and some problems in astronomy about some peculiar motions of distant star formations. According to Eq. (19), the ratio between P_S (related to the mass) and P_P (related to the dynamics of any object - particle, atom, molecule or solid body) has a preferable value defined by the fine structure constant. When regarded as an optimal tendency, this ratio might

have a signature even in the galactic rotational curves and the evolution of the galaxies from S0 to SB or Sc branch. This conclusion comes from the BSM-SG analysis of the galactic rotational curves for different types of galaxies using data provided by Rubin et al. [27] and other researchers.

One indication of inertial interactions between the rotating massive object and CL space is the preferable orientation of the polar axes of the solar planets in respect to the galactic rotation of the solar system, as shown in Fig. 13. The effect is consistent with the inertial mass anomaly observed in spinning gyroscopes [28].

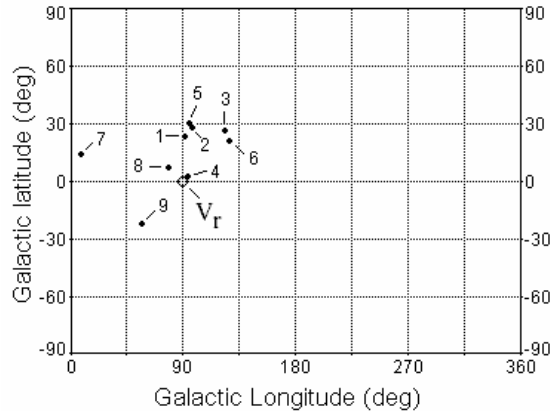


Fig. 13. Solar vector V_r and North polar axes of the solar system planets in galactic coordinates (data from planetary datasheets). 1- Mercury, 2 – Venus, 3 – Earth, 4 – Mars, 5, Mars, 6 – Saturn, 7, Uranus, 8 – Neptun, 9 – Pluto

A new vision about the Universe

The individual galaxies have their own cycle of active life (observable) and hidden not observable phases. The hidden phases are not observable because the surrounding space is completely empty with no physical properties and not transmitting EM waves. During the hidden phases the atomic matter including elementary particles recycle to lower formations after which a crystallization of new elementary particles takes place. The transition events between the observable and hidden phases are the galactic collapse and galactic birth, which have detectable signatures – the observable Gamma Ray Bursts (GRB). Some galactic matter, escaping the collapse, forms the Globular Clusters and “Irregular galaxies”, such as Sagittarius. During the formation of the prisms (subelementary particles) all galactic matter (the mass of which is detectable during the galactic active life) participates. Since the total galactic mass of the galaxies is different, prisms from different formations will have a

small variation of their length to radius ratio. Then a photon emitted and detected in one and a same galactic space will not have a cosmological redshift (the environment preserve the optimal quantum interactions). However, a photon passing through different galactic spaces will exhibit a small energy loss due to refurbishing of its wavetrain in the boundary zones between the galaxies. The observable effect is a galactic readshift, which is not of Doppler origin. If expressing the difference between two galactic spaces as an average quasirefractive index, \tilde{n} , the ratio between the observed and emitted wavelength of the photon is $\lambda_i/\lambda_0 = (\tilde{n})^N$, which leads to the expression

$$(\tilde{n})^N = z + 1 \tag{24}$$

where: z – is the cosmological redshift from N crossed galactic boundaries

One detectable signature of this phenomenon is the Lyman Alpha Forest, providing an estimate of the number of crossed boundaries. Then the new corrected distance to a galaxy with a redshift of z is given by

$$r = \frac{c^2 \ln(\tilde{n})}{\tilde{L}H_0} \int_0^z \frac{x}{\ln(1+x)} dx \tag{25}$$

where: \tilde{n} - is determined from the mean density of the Lyman alpha forest lines for signal emitted by a distant quasar, \tilde{L} - an average distance between the neighboring galaxies, H_0 – Hubble constant, c – velocity of light

Figure 14 shows a Hubble plot from experimental data for z up to 1.75 [28], while Fig. 15 shows the theoretical plot of Eq. 20, normalized to the constant $(c^2 \ln(\tilde{n})/\tilde{L}H_0)$.

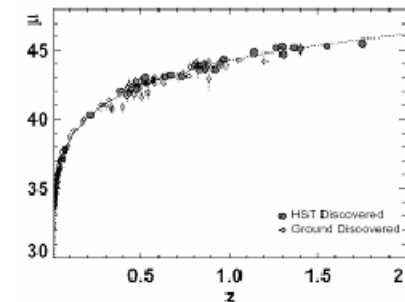


Fig. 14

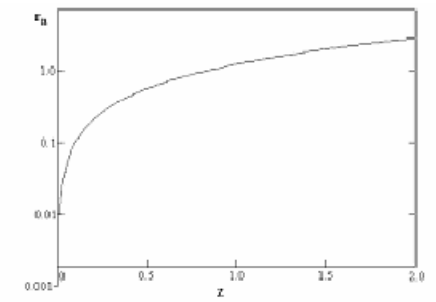


Fig. 15

Conclusion: The space in observable Universe is inhomogeneous, so the observed galactic redshift is not of Doppler origin. The Universe is stationary.

A new interpretation of the Einstein's equation $E = mc^2$

The mass is a parameter of a structural formations from indestructible Fundamental Particles, so it is not equivalent to matter. Consequently, annihilation or creation of matter (Fundamental Particles) is impossible. Then the correct interpretation of the Einstein's equation is as following:

$mc^2 \rightarrow E$ - valid for particle disintegration (in particle collision experiments) or hiding of the positron's mass inside of the electron structure

$E \rightarrow mc^2$ - valid for creation of a virtual particle (not possessing matter)

$E \rightleftharpoons mc^2$ - valid for the binding energy in the atomic nuclei, as a result of small change of the CL space node distance in presence of matter.

The new concept of the physical vacuum leads to important predictions, discussed in Chapter 13 of BSM-SG. The most important of them are: (1). Unveiling a hidden space energy of non EM type, which is the primary source of the nuclear energy, (2) Predicting a new method for supercommunication by using not well investigated so far longitudinal waves, (3) Predicting the possibility for control the gravitational and inertial mass of material object, by proper modulation of the physical vacuum parameters.

Summary and conclusions: The new concept of the physical vacuum leads to a new vision about space, time, matter, energy and gravitation, while unveiling a different picture about the microcosmos and Universe.

- The common origin of the observed world from micro to macro scale is explainable by a physical model of two indestructible Fundamental Particles with parameters associated to Planck's scale and interactions governed by an inverse cubic law called a Law of Supergravitation
- The Supergravitational law is the most fundamental law in Nature.
- The physical vacuum contains underlying superfine material structure. It defines space-time, Quantum Mechanical and Relativistic properties of the space and it is responsible for propagation of the Gravitational, Electrical and Magnetic fields.
- The fundamental laws of Physics are embedded in the superfine material structures of the physical vacuum and the elementary particles.

- The fine structure constant is embedded in the basic level of matter organization, while its signature is propagated in all upper levels.
- The galactic redshift is not of Doppler type. The Universe is stationary.
- Every galaxy has its own cycle comprised of a visible active life and a hidden phase of matter recycling. The Gamma Ray Bursts (GRB) are detectable signatures of a birth or collapse of a galaxy. The Globular Clusters and some irregular galaxies (like Sagitarius) are remnants from the previous galactic life, which have escaped the collapse.
- The space contains hidden (not EM type) energy, which is a primary source of the nuclear energy. Alternative methods for access to this energy are possible (Chapter 13 of BSM-SG).
- The Gravitational and inertial mass of a solid body could be manageable – a promising opportunity for distant space travels (Chapter 13).

**References:**

1. N. A. Zhuck et al, Quasars and the large-scale structure of the Universe, Spacetime & Substance, v. 2 No. 5 (10), p.193-210, (2001)

2. J. C. Maxwell, *A Treatise on Electricity and Magnetism*, v. 2 (Dover Publications, N. Y. p. 493, (1954))
3. A. Einstein, *Sidelights on Relativity*, translated by G. Jeffery & W. Perrett, Methuen & Co. Ltd, London, (1922)
4. D. C. Miller, The Ether-Drift Experiment and Determination of Absolute Motion of the Earth, *Review of Modern Physics*, 5, 203-242, (1933)
5. G. F. Smoot et al., Detection of Anisotropy in the Cosmic Blackbody Radiation, *Physical Review Letters*, 39, No 14, 898-901, (1977)
6. R. A. Muller, The Cosmic Background Radiation and the New Aether Drift, *Scientific American*, 238, 64, (1978)
7. S. Marinov, Measurement of the Laboratory's Absolute velocity, *General Relativity and Gravitation*, 12, 57-66, (1980)
8. S. Marinov, The interrupted "rotating disc" experiment, *J. Phys A: Math. Gen.*, 16, 1885-1888, (1983)
9. E. W. Silvertooth, Experimental detection of the ether, *Speculations in Science and Technology*, 10, No 1, 3-7, (1986)
10. S. Marinov, Экспериментальные нарушения принципов относительно сти, эквивалентности и сохранения энергии, *Физическая мысль России*, No 2, 52-57, (1995)
11. C. Monstein and J. P. Wesley, Solar System Velocity from Muon Flux Anisotropy, *Apeiron*, 3, No. 2, 33-37, (1996)
12. R. T. Chill and Kirsty Kitto, Michelson-Morley Experiments Revisited and the Cosmic Background Radiation Preferred Frame, *Apeiron*, 10, No 2, 104-1017, (2003)
13. M. Consoli and E. Costanzo, From Classical to modern ether-drift experiments: the narrow window for a preferred frame, *Physics Letters A*, 333, 355-363, (2004), also arXiv:astro-ph/0601420 v. 2, (2006)
14. S. Sarg, *Basic Structures of Matter* (first edition 2002, second edition, 2002) electronic archives, National Library of Canada
15. S. Sarg, *Basic Structures of Matter – Supergravitation Unified Theory*, Trafford Publishing, Canada, 2006, ISBN 141208387-7 (www.trafford.com/06-01421).
16. S. Sarg, New approach for building of unified theory, <http://lanl.arxiv.org/abs/physics/0205052> (May 2002)
17. S. Sarg © 2001, Atlas of Atomic Nuclear Structures, monograph, <http://www.nlc-bnc.ca/amicus/index-e.html> (April, 2002), (AMICUS No. 27106037); Canadiana: 2002007655X; ISBN: 0973051515, LC Class: QC794.6*; Dewey: 530.14/2 21
18. S. Sarg, Brief introduction to Basic Structures of Matter theory and derived atomic models, *Journal of Theoretics* (Extensive papers), January, 2003; <http://www.journaloftheoretics.com>

19. S. Sarg, Atlas of Atomic Nuclear Structures according to the Basic Structures of Matter Theory, *Journal of Theoretics* (Extensive papers, March, 2003); <http://www.journaloftheoretics.com>
20. S. Sarg, Application of BSM atomic models for theoretical analysis of biomolecules (with three formulated hypotheses), *Journal of Theoretics*, May 2003; <http://www.journaloftheoretics.com>
21. S. Sarg, A Physical Model of the Electron according to the Basic Structures of Matter Hypothesis, *Physics Essays*, 16 No. 2, 180-195, (2003); <http://www.physicsessays.com>
22. S. Sarg, New vision about a controllable fusion reaction with efficient energy yield, ISBN 0973051523, (AMICUS No 27276360), (2002)
23. S. Sarg, Basic Structure of Matter Hypothesis Based on an Alternative Concept of the Physical Vacuum (poster report), "Physics for the Third Millennium" Conference, organized by NASA, Huntsville AL, USA, 5-7 Apr 2005.
24. S. Sarg, Basic Structures of Matter Hypothesis Based on an Alternative Concept of the Physical Vacuum, 12th Annual conference of Natural Philosophy Alliances, 23-27 May 2005, Storrs, CT, USA.
25. S. Sarg, *Beyond the Visible Universe*, Helical Structures Press, Canada, 2004, ISBN 0973051531
26. A. I. Zakazchikov, The evolution of the vision about Ether, Proc. Of VIII International Scientific Conference, "Space, Time, Gravitation", 16-20 Aug 2004, St. Petersburg, Russia (p. 96-110)
27. Rubin et al., Rotation velocities of 16 Sa galaxies and a comparison of Sa, Sb and Sc rotation properties, *Astrophysical Journal*, 289, 81-104, (1985)
28. K. Gerber, R. Merritt and E. Delters, Gyro Drop Experiment <http://depalma.pair.com/gyrodrop.html>